High-frequency measurements of dissolved organic carbon quantity and quality in a headwater catchment

Benedikt J. Werner[1], Andreas Musolff[1], Oliver J. Lechtenfeld[2], Gerrit H. de Rooij[3], Marieke R. Oosterwoud[1], Jan H. Fleckenstein[1]

5 [1]Department Hydrogeology, Helmholtz Centre for Environmental Research - UFZ, Leipzig, 04318, Germany
[2]Department Analytical Chemistry, Research group BioGeoOmics, Helmholtz Centre for Environmental Research - UFZ, Leipzig, 04318, Germany
[3]Department Soil System Sciences, Helmholtz Centre for Environmental Research - UFZ, Halle, 06120, Germany

10 *Correspondence to*: Benedikt Werner (benedikt.werner@ufz.de)

Abstract. Increasing dissolved organic carbon (DOC) exports from headwater catchments impact the quality of downstream waters and pose challenges to water supply. The importance of riparian zones for DOC export from catchments in humid, temperate climates has generally been acknowledged, but the hydrological controls and biogeochemical factors that govern mobilization of DOC from riparian zones remain elusive. A one-year high-frequency (15 minutes) dataset from a headwater

15 catchment in the Harz Mountains (Germany) was analyzed for dominant patterns in DOC concentration (C_{DOC}) and optical DOC quality parameters $SUVA_{254}$ and $S_{275-295}$ (spectral slope between 275 nm and 295 nm) on event and seasonal scale. Quality parameters and C_{DOC} systematically changed with increasing fractions of high-frequency quick flow (Q_{hf}) and antecedent hydroclimatic conditions, defined by the following metrics: Aridity Index (AI_{60}) of the preceding 60 days, mean temperature (T_{30}) and discharge (Q_{30}) of the preceding 30 days and the quotient T_{30}/Q_{30} which we refer to as discharge-

20 normalized temperature (DNT_{30}). Selected statistical regression models for the complete time series (R^2= 0.72, 0.64 and 0.65 for C_{DOC}, $SUVA_{254}$ and $S_{275-295}$, resp.) captured DOC dynamics based on event (Q_{hf} and baseflow) and seasonal-scale predictors (AI_{60}, DNT_{30}). The relative importance of seasonal-scale predictors allowed for the separation of three hydroclimatic states (warm & dry, cold & wet and intermediate). The specific DOC quality for each state indicates a shift in the activated source zones and highlights the importance of antecedent conditions and its impact on DOC accumulation and

25 mobilization in the riparian zone. The warm & dry state results in high DOC concentrations during events and low concentrations between events and thus can be seen as mobilization limited, whereas the cold & wet state results in low concentration between and during events due to limited DOC accumulation in the riparian zone. We conclude that the high concentration variability of DOC in the stream can be explained by only a few controlling variables. These variables can be linked to DOC source activation by discharge events and the more seasonal control of DOC production in riparian soils.

1 Introduction

Over the last decades dissolved organic carbon (DOC) exports from catchments have notably increased (Evans et al., 2005; Freeman et al., 2001; Monteith et al., 2007), thereby redistributing carbon pools of inland waters and affecting the global carbon cycle (Battin et al., 2009; Cole et al., 2007; Hope et al., 1994). Increased riverine exports of DOC from catchments can impair the downstream water quality and aquatic ecology (Hruška et al., 2009). The impact of DOC on downstream waters is not only related to the concentration (C_{DOC}) in the water, but also to the specific chemical composition of DOC, also referred to as DOC quality. Depending on the DOC quality, the growth of microorganisms is affected (Ågren et al., 2008) by different provision of thermodynamically available energy (Stewart and Wetzel, 1981). Berggren and del Giorgio (2015) pointed out that shifts in DOC quality could dramatically change the patterns of aquatic microbial metabolism resulting in altered ecosystem functioning. DOC increases the costs of water purification (Alarcon-Herrera et al., 1994): Both DOC quantity and quality determine the coagulant dose in water treatment (Sharp et al., 2006; Vik and Eikebrokk, 1988), as well as the risk of toxic disinfection by-products during chlorination (Vik and Eikebrokk, 1988). Thus, the dynamics of the amount and quality of DOC exported from catchments are of growing concern in water quality and environmental management. In order to provide water managers with guidelines to mitigate the negative effects of DOC in streams and lakes, we need to better understand the mechanisms that drive DOC mobilization and export and its respective changes in quality.

The observed long-term increases in DOC export have been related to declining atmospheric acid deposition and rising temperatures (Evans et al., 2005), climate and land use change (Chantigny, 2003), decreasing nitrogen deposition (Musolff et al., 2017), and reduction in ionic strength (Hruška et al., 2009). Monteith et al. (2007) explained rising C_{DOC} by decreases in sulphur and sea salt deposition and the catchment sensitivity to acid deposition (represented by median Ca^{2+} and Mg^{2+} concentrations).

Most of the riverine DOC in temperate humid and boreal catchments is derived from terrestrial sources and is mobilized at the terrestrial-aquatic interface (Laudon et al., 2012; Ledesma et al., 2018; Musolff et al., 2018). Besides wetlands, the riparian zone is seen as a dominant source zone of DOC, defining potential DOC export loads and their temporal patterns (Ledesma et al., 2015; Musolff et al., 2018). Here, DOC can be mobilized from shallow organic soil layers when event runoff is generated from those parts of the soil profile. Soil moisture and rain intensity, but also local hydromorphology influence the extent of overland and lateral subsurface flows in the riparian zone, which activate varying sources of DOC of different quality (Blaen et al., 2017; Ledesma et al., 2015). Thus, differences in DOC quality observed during varying runoff conditions have been used to characterize source zone activation in smaller watersheds (Hood et al., 2006; Sanderman et al., 2009).

Storm events typically show high variability in C_{DOC} and DOC quality (Bishop et al., 1990; Strohmeier et al., 2013) and generate most of the overall DOC loads exported from catchments (Buffam et al., 2001; Hope et al., 1994). Daily precipitation and amount of discharge (Bishop et al., 1990) were found to be event-scale drivers whereas seasonality in

discharge (Ågren et al., 2007), soil wetness (Lepisto et al., 2014) and average daily temperature (Roth et al., 2015) control intra-annual DOC variability (Ågren et al., 2007; Hope et al., 1994; Köhler et al., 2009).

Although individual storms play a crucial role in DOC exports, most studies to date have only focused on temporally aggregated data (Köhler et al., 2008) and the seasonal time scale with little or no consideration of the event-scale variability of DOC quantity and quality. Recent years have seen significant advances in sensing technologies for high-frequency in situ concentration measurements (Rode et al., 2016; Strohmeier et al., 2013) as well as spectral and analytical methods to characterize DOC composition (Herzsprung et al., 2012; Raeke et al., 2017; Roth et al., 2013). Combining information on DOC quantity and quality at temporal resolutions capable of capturing the dynamics within hydrologic events provides an opportunity to significantly improve our mechanistic understanding of DOC mobilization, transport, and ultimately export from catchments (Berggren and del Giorgio, 2015; Creed et al., 2015; Köhler et al., 2009; Strohmeier et al., 2013). Studying the DOC mobilization mechanisms at the riparian interface at time-scales ranging from individual events driven by heavy rain or snowmelt to the potentially decadal response to the long-term changes described above are therefore a prerequisite for adequate modelling approaches and management guidelines.

The main objective of this paper is to better understand how event-scale DOC quality dynamics in headwater streams are linked to DOC mobilization processes in the riparian zone and how high-frequency measurements of C_{DOC} and spectral properties can be utilized to identify and quantify the key controls of DOC export from event to seasonal time scales. We therefore i) evaluate the variability of concentration and quality of DOC during events and on a seasonal scale based on high-frequency measurements, ii) extract the most decisive factors and controls for C_{DOC} and quality variability, and iii) synthesize them in a quantitative-statistical and finally conceptual model of DOC export.

To this end, a high-frequency dataset on C_{DOC} and DOC quality from a first-order catchment in Central Germany was evaluated in terms of key controlling variables such as discharge, temperature and antecedent wetness conditions. The dominant drivers for understanding seasonal- and event-scale variability of C_{DOC} and quality were extracted and assessed (a) by a correlation analysis of intra-annual variations (seasonal scale), and (b) by an analysis of the individual discharge events throughout the year (event scale), respectively. In a final step (c), these drivers were interpreted mechanistically based on a multiple linear regression analysis covering the entire study period.

2 Materials and Methods

2.1 Study site

Measurements were conducted in a headwater catchment of the Rappbode stream (51°39'22.61"N 10°41'53.98"E, Fig. 1) located in the Harz Mountains, Central Germany. The Rappbode stream flows into a large drinking water reservoir. Downstream of the reservoir it flows into the river Bode, and eventually discharges (via the rivers Saale and Elbe) into the North Sea. The investigated part of the catchment has an area of 2.58 km² and a drainage density of 2.91 km km^{-1}. The catchment is mainly forested with spruce and pine trees (77%), the remaining area is covered with grass (11%) and other

vegetation (12%). Elevation ranges from 540 to 620 m above sea level; the mean topographic slope is 3.9°. The 90th

percentile of the topographic wetness index as a measure for the extent of riparian wetlands in the catchment (Musolff et al.,

2018) is 8.53 (median 6.77). The geology at this site consists mainly of graywacke, clay schist and diabase (Wollschläger et

al., 2016). Soils in the vicinity of the Rappbode spring are dominated by peat. Overall, one quarter of the catchment is

5   characterized by groundwater-influenced humic gleysols and stagnic gleysols, which are mainly found in the riparian zones.

Riparian soils were mapped next to the Rappbode stream, 2 km downstream of the spring. At this site, topsoil layer (A

horizon) thickness in a transect (Fig. 1) was 17.7 cm +/- 2.4 cm on average (n = 27) up to 25 m off the stream. The study site

has a temperate climate (Kottek et al., 2006), with a long-term mean temperature of 6.0 °C and mean annual precipitation of

831 mm (Stiege weather station 12 km away from the study site, data provided by the German Weather Service DWD).

10   **2.2 Data basis**

An overview of all variables utilized for site description and regression modeling as well as descriptive statistics of these

variables are given in Table 1.

2.2.1 Monitoring of response variables: DOC concentration and quality

We used in situ absorption spectroscopy to determine DOC quantity and quality. DOC quality can be characterized by

15   specific metrics based on the light absorbing properties of dissolved organic compounds such as $SUVA_{254}$ (specific UV

absorbance at 254 nm) (Weishaar et al., 2003) and the spectral slope between 275 and 295 nm, denoted $S_{275-295}$ (Helms et al.,

2008). General patterns of these metrics can be used to infer information on the origin (autochthonous vs. allochthonous,

molecular weights), processing (photobleaching and microbial degradation change aromaticity) (Helms et al., 2008) and

source zone characterization of DOC in riparian zones (Eran et al., 2006; Hutchins et al., 2017; Sanderman et al., 2009).

20   An UV-Vis probe (Spectrolyzer, scan Messtechnik GmbH, Austria) was installed in the stream (Fig. 1) in April 2013 to

measure light absorption spectra from 220 nm to 720 nm in 2.5 nm steps every 15 min. There is a data gap from 11

December 2013 until 14 January 2014 due to general maintenance and recalibration of the UV-Vis probe in the laboratory.

Other gaps from 18 November 2013 until 27 November 2013 and from 01 September 2014 until 17 September 2014 were

due to a probe failure; accordingly values were excluded a priori. Overall, the UV-Vis dataset comprises 42,427

25   measurements. For a description of fouling correction, onsite probe maintenance and water sampling refer to S1 in the

supplements.

After fouling correction, UV-Vis measurements were used to derive C_{DOC}, $SUVA_{254}$ and $S_{275-295}$. For validation and

calibration of C_{DOC} and $SUVA_{254}$, 28 grab samples were used that have been taken biweekly from the stream to measure the

specific absorption coefficient at 254 nm (SAC$_{254}$ (UVT P200, Real Tech Inc., Canada) and C_{DOC} (DIMATOC® 2000,

30   Dimatec Analysentechnik GmbH, Germany). A continuous time series of C_{DOC} from the UV-Vis spectra was created using

partial least squares regression (PLSR) to the 28 concentration values via the R package pls (Mevik and Wehrens, 2007).

The PLSR proved to robustly work with a large number of predicting variables and strong collinearities (Musolff et al.,

2015; Vaughan et al., 2017). The procedure generally followed the method described in Etheridge et al. (2014) using all turbidity-compensated spectra within a single regression model, chosen by 10-fold cross validation of the training data set. Through this method, C_{DOC} was defined by a local combination of several wavelengths that proved to yield better results than the predefined global settings provided by the probe (Vaughan et al., 2017).

5 $SUVA_{254}$ was calculated by dividing the spectral absorption coefficient at 254 nm (SAC_{254}) by the PLSR-derived C_{DOC} values. The resulting $SUVA_{254}$ values were then validated (but not calibrated) by the 28 $SUVA_{254}$ values derived from the manual SAC_{254} measurements in the field and the associated lab C_{DOC} measurements.

As a second quality metric $S_{275-295}$ was estimated from the fouling-corrected adsorption spectra as described in Helms et al. (2008): A linear regression model was fitted for each time step to the logarithms of the absorption coefficients between 275

10 and 295 nm to derive the slope $S_{275-295}$.

2.2.2 Predictor variables: Stream level and discharge, evapotranspiration and antecedent wetness condition

Discharge Q_{tot} was calculated from a stage-discharge relationship, which was established based on the 15 min stage readings from a barometrically compensated pressure transducer (Solinst Levellogger, Canada) and biweekly manual discharge measurements using an electromagnetic flow meter (n = 42; MF pro, Ott, Germany).

15 Manually measured discharge maximum was 0.39 m³ s^{-1} at a water level of 83.8 cm. Ungauged water levels above this value and the associated discharges were extrapolated from the stage-discharge relationship and found to be within a valid range when comparing to modelled discharge from the mesoscale hydrological model mHM (Mueller et al., 2016; Samaniego et al., 2010). A hydrograph separation into event and baseflow components was applied following the method described by Gustard and Demuth (2009). Total discharge Q_{tot} was partitioned into a high-frequency quick flow (Q_{hf}) component, active

20 during events and a low frequency component representing base flow (Q_b). To derive the baseflow hydrograph, local flow minima of non-overlapping five-day periods were selected and linearly connected to each other using the lfstat package (Koffler et al., 2016) in R (R-Core-Team, 2017). If the baseflow hydrograph exceeded the actual flow, it was constrained to equal the observed hydrograph of Q_{tot}. Events were then extracted by subtracting Q_b from Q_{tot}.

To characterize ambient weather conditions, a weather station (WS-GP1, Delta-T, United Kingdom) placed about 250 m

25 northwest of the UV-VIS probe provided data on air temperature (T), air humidity, wind direction and speed, solar radiation, and rainfall (P) at a 30 min interval. Measurements between 21 May 2013 and 26 June 2013 were at an hourly interval.

Potential evapotranspiration (ET_P) was calculated on an hourly basis from the weather data after Penman-Monteith (Allen et al., 1998). The antecedent aridity index (AI_t) gives an estimate of the water balance in the last t days and equals the aridity index for longer time periods given by Barrow (1992). Accordingly, AI_{60} was derived for the measurement period by

30 dividing the cumulative sum of precipitation over the last 60 days (P_{60}) by the cumulative sum of ET_P of the last 60 days ($ET_{P,60}$).

The discharge-normalized temperature of the preceding 30 days (DNT_{30}) was calculated by dividing the mean air temperature of the preceding 30 days by the mean discharge of the preceding 30 days. DNT_{30} gives an estimate of the ratio

between temperature (that controls soil DOC production, e.g. Christ and David (1996)) and discharge (that controls DOC export, e.g. Hope et al. (1994)) in the last 30 days and therefore can potentially be related to the state of DOC storage in top soils.

In order to obtain a complete dataset for all variables, observations were excluded a priori according to the UV-Vis data gaps
5   from 18 November 2013 until 27 November 2013, 11 December 2013 until 14 January 2014 and 01 September 2014 until 17 September 2014

2.3 Statistical analysis

Evaluation of the variable's predictive power was done for the entire dataset as well as for separated discharge events. Descriptive statistical tools were applied using the software R (R-Core-Team, 2017). Spearman's rank correlation (r_s) was
10   used to look for significant relations of C_{DOC} and DOC quality with potential controlling variables, since concentration, discharge and solute loads in river systems usually have lognormal probability distributions while C-Q relationships can be described by power law functions (Jawitz and Mitchell, 2011; Köhler et al., 2009; Rodríguez-Iturbe et al., 1992; Seibert et al., 2009).

2.3.1 Event-scale analysis

15   Consequently, concentration-discharge (C-Q) relationships were characterized and quantified in log-log space for the event analysis. Since metrics of DOC quality are typically normally distributed (Guarch-Ribot and Butturini, 2016; Sanderman et al., 2009), relationships between quality and Q_{tot} were analyzed in semi-log space. According C-Q and quality-Q relationships for each runoff event (n = 38) were represented by combinations of multiple linear regression models with Q_{tot}, Q_b and Q_{hf} and their log transformations as predictors. The best overall combination of two variables for the prediction of
20   events was chosen according to the best mean R² of all 38 single models. Subsequently, the 38 triplets of intercepts and regression coefficients of the best event model (e.g. log(C_{DOC}) ~ a log (Q_{hf}) + b Q_b +z) were extracted for further analysis.

2.3.2 Seasonal-scale analysis

To explain seasonal variations in the event analysis, the 38 regression coefficient triplets were correlated with seasonal-scale antecedent key controlling variables. Variables which showed strong correlations were added in different combinations to
25   the existing event model as potential predictors for seasonal variations in addition to the event-scale variance. Here, dependent variables C_{DOC}, $SUVA_{254}$ and $S_{275-295}$ models always used the same predictor variables. The interaction between two predictor variables was generally used for modelling. This implies that the measured environmental variables influence each other and thus cause a non-additive effect on the dependent variable. Here, we write interaction terms as the product between the two interacting variables (variable1 × variable2). As recommended by Marquardt (1970) and Menard (2001),
30   multicollinearity of predictors (variables and interaction terms) was taken into account based on the variance inflation factor (VIF; R package car (Fox and Weisberg, 2011)):

$$VIF_i = \frac{1}{1-R_i^2} > 10 \qquad\qquad (1)$$

where VIF_i is the variance inflation factor for every predictor variable and interaction i in the complete model, predicted by multiple linear regression from the remaining predictor variables of the complete model. R_i^2 is the corresponding coefficient of determination. Variables and interactions were excluded from the complete model if Eq. (1) holds for variable i.

5 Akaike's Information Criterion (AIC) and R² were used for model selection and validation. Five-fold cross-validation was applied to estimate the prediction error. Once the most valid model was selected, the predictive power of the chosen predictors for the different models of C_{DOC} and DOC quality was tested. On the one hand, partial models were built by stepwise dropping the least influencing predictors according to AIC and by comparing the subset of event-scale predictors with the subset of seasonal-scale predictors.

3. Results

3.1 Monitoring of DOC and hydroclimatic parameters

The basic statistics of UV-Vis-derived C_{DOC} and DOC quality as well as hydroclimatic variables throughout the 1.5-year measurement period are given in Table 1.

The amount of precipitation during 2013 (665 mm) and 2014 (682 mm) was close to the long-term annual mean at the

15 nearest weather station. Discharge shows event-type variability but followed in general the hydrological year, with lowest values in late summer and highest values in spring (Fig. 2a). Highest discharge was 1.98 m³ s⁻¹ during snowmelt on 27 April 2014. With a coefficient of variation (CV) much higher than 1, the discharge regime can be described as erratic (Botter et al., 2013), indicating the importance of the quick flow component for discharge in the Rappbode catchment. Consequently, the variability of Q_{hf} mostly follows Q_{tot}, but without the seasonal baseflow trends. A total number of 38 discharge events have

20 been separated by discharge partitioning, yielding an average frequency of 0.086 d⁻¹. A dry period occurred from 14 June 2013 to 23 July 2013, which resulted in a steady decline in discharge during that time (Fig. 2).

Air temperature exhibited strong seasonal patterns and was comparable to the seasonal mean at the nearest station. Daily

25 sums of ET_P peaked in summer whereas ET_P in autumn and winter reached the minimum. The general pattern follows a typical seasonal sinusoidal shape (not shown).

The aridity index AI_{60} indicates a general wet climate with higher precipitation than potential evapotranspiration. AI_{60} peaked in winter whereas minimum values occurred in summer during the drought and in winter during the freezing period (Fig. 2b). Summer precipitation has only little impact on AI_{60}. With a CV of 0.74, ET_{P60} generally has more influence on the

30 variability of AI_{60} than P_{60} (CV = 0.53).

DNT_{30} peaked in summer whereas minimum values occurred in winter (Fig. 2b). Generally, Q_{30} (CV = 0.89) has more influence on the variability of DNT_{30} than T_{30} (CV = 0.53). Precipitation events in cold periods have only little impact on DNT_{30} and peaks due to precipitation are barely detectable since P_{30} on average covers 2.6 events.

C_{DOC} based on the PLS regression fits well to the DOC concentration measured in the lab (R^2 = 0.97, residual standard error:

5   0.68 mg L^{-1}) (Fig. 2c). The maximum deviation of PLS-based from lab-measured C_{DOC} of 1.7 mg L^{-1} occurs on 24 July 2013. We argue that the PLSR predicts the average characteristic composition of DOC rather well but hardly accounts for changes in DOC quality and thus spectral properties due to extreme situations (Vaughan et al., 2017). Accordingly, C_{DOC} and hence calculated $SUVA_{254}$ values less match the manual measurements during such situations, leading to an overall R^2 of 0.5 for $SUVA_{254}$ values, but removing three measurements taken during longer dry periods (09 July 2013, 04 September 2013, 23

10   July 2014) increases overall R^2 to 0.73.

There are no laboratory values available to verify $S_{275-295}$ calculations, but calculated values are in the same magnitude as reported in the literature (Helms et al., 2008; Spencer et al., 2012).

C_{DOC}, $SUVA_{254}$ and $S_{275-295}$ exhibit pronounced event-type variability over the entire year (Fig. 2c - e). In winter months, DOC was low in concentration, but had a distinct quality signature with high $S_{275-295}$ and $SUVA_{254}$ values (Fig. 2c - e).

15   Furthermore, only small fluctuations of concentration and quality were observed in winter. Summer months showed minimum C_{DOC}, $SUVA_{254}$ and $S_{275-295}$ values in both years during baseflow, but also the most distinct C_{DOC} and quality variations during discharge events. Late summer and autumn C_{DOC} were different between 2013 and 2014 with a pronounced temporal variability in 2014 compared to rather small fluctuations in 2013. DOC quality characteristics were similar in autumns of both years, exhibiting an average range compared to the entire measurement period. During events in spring and

20   autumn, $S_{275-295}$ and $SUVA_{254}$ remained at a constant level, indicating the export of DOC of similar composition.

Exported DOC loads (Table 1) peaked during high discharge events during spring and autumn and closely follow the hydrograph (Fig. S1). Accordingly, the CV of the load is closer to that of the discharge than to the CV of DOC (Table 1). Maximum DOC export was found during the discharge event on 27 April 2014 with rates of up to 18.6 g s^{-1}. Although events in drier summer months show stronger concentration fluctuations, exported loads remain low.

3.2 Correlation analysis

Table 2 shows correlations for the entire dataset of C_{DOC} and DOC quality with possible controlling variables (T, Q, AI, DNT) aggregated at different time steps. We use Spearman's rank (r_s) correlation to determine the direction and strength of

30   relationships between variables.

C_{DOC} correlates strongest with $SUVA_{254}$, but r_s between C_{DOC} and $S_{275-295}$ and between $S_{275-295}$ and $SUVA_{254}$ is markedly smaller.

Correlations of Q_{tot} with $S_{275\text{-}295}$ are stronger than Q_{tot} with $SUVA_{254}$ and C_{DOC}, respectively. In comparison to Q_{tot}, correlations with Q_{hf} are markedly higher for C_{DOC} and $SUVA_{254}$, but lower for $S_{275\text{-}295}$. On the other hand, when relating C_{DOC} and metrics of quality to the baseflow fraction of discharge Q_b, r_s is close to 0 for C_{DOC} and $SUVA_{254}$, but 0.61 for $S_{275\text{-}295}$. C_{DOC} and quality further correlate with antecedent discharge, temperature, discharge normalized temperature (DNT_{30}) and aridity index

5 ($AI_{6, 14, 60}$). C_{DOC} and $SUVA_{254}$ correlate best with AI_6, whereas $S_{275\text{-}295}$ correlate with T_{30}, Q_{15}, Q_{30}, DNT_{30} and AI_{60}.

3.2.1 Event-scale analysis

High coefficients of determination (R^2) between C_{DOC} and DOC quality metrics with Q_{hf} and partly with Q_b underline the prominent role of discharge and its different time scales for DOC variability. Consequently, quantifying DOC mobilization

10 for a range of individual events may provide information for better understanding direction, shape and strength of C-Q relationships. The analysis of the response of C_{DOC} and DOC quality to discharge events covers 47.5% of the entire time series. The relationship between C_{DOC} and Q_{tot} during events resembles a segmented slope in log-log space (Fig. S2a), similar to the C-Q behavior described by Moatar et al. (2017), which inhibits a proper parameterization by the usually applied simple power law regression. However, when detrending the discharge by baseflow subtraction, the resulting C_{DOC}-Q_{hf}

15 relationship is more linear in log-log space (Fig. S2b). This behavior occurs for the event-scale discharge variability of the entire dataset. Hence, independent variable $\log(C_{DOC})$ is best predicted by a combination of both discharge components during single discharge events. For DOC quality metrics $SUVA_{254}$ and $S_{275\text{-}295}$ we applied a similar model to predict the non-transformed independent variables:

$$Y = a\,\log(Q_{hf}) + b\,Q_b + z \qquad\qquad (2)$$

20 where Y is $\log(C_{DOC})$, $SUVA_{254}$ or $S_{275\text{-}295}$, resp.; a, b are regression coefficients and z is the intercept.

We applied Eq. (2) to 38 individual discharge events. The mean R^2 of all $\log(C_{DOC})$ models (one model for each discharge event) is 0.84 (±0.15). Respective mean R^2 values for $SUVA_{254}$ and $S_{275\text{-}295}$ were 0.83 (±0.14) and 0.64 (±0.26). Performance of the models is always better than a simple linear regression with $\log(Q_{tot})$ (mean R^2 for $\log(C_{DOC})$, $SUVA_{254}$ and $S_{275\text{-}295}$ is 0.76 (±0.16), 0.70 (±0.15) and 0.50 (±0.26), respectively). R^2 of the models from Eq. (2) varies over time (Fig. 3). Dependent

25 variables $\log(C_{DOC})$ and $SUVA_{254}$ show a similar behavior with maximum R^2 in autumn and winter and minimal R^2 values in spring and summer (Fig. 3a and b). R^2 of the $S_{275\text{-}295}$ models show a different and less consistent pattern with higher variability between events than C_{DOC} and $SUVA_{254}$ models (Fig. 3c). In comparison to C_{DOC} and $SUVA_{254}$, $S_{275\text{-}295}$ values in winter and spring events have a systematically lower R^2.

Coefficients of C_{DOC} and DOC quality models vary between the events (Fig. 3 a-c). Coefficient a (regression coefficient of

30 $\log(Q_{hf})$) shows low but more systematic variations over time, represented by a smaller CV in comparison to z and b (mean $CV_a = 0.76$, mean $CV_z = 2.58$, mean $CV_b = 5.30$ of the C_{DOC}, $SUVA_{254}$ and $S_{275\text{-}295}$ models). High a values indicate a stronger increase in C_{DOC} and change in quality of DOC with an increase in Q_{hf}, whereas small a values indicate only little change

with increasing Q_{hf}. All three models show a distinct change in a from dry summer to autumn 2013. The summer months generally show the strongest variability in model coefficient, meaning that C_{DOC} and DOC quality reacted strongly and more variable to the comparable small discharge events. Winter months in contrast show least variability in model coefficient a indicating a more homogeneous reaction to discharge in this time of the year. Baseflow and intercept model coefficients b

5 and z have a similar, less distinct, pattern for all three models with higher parameter variability in summer compared to the other months.

3.2.2 Seasonal-scale analysis

A correlation analysis of the model coefficients a, b and intercept z was performed to identify the variables that explain their
10 temporal dynamics (Table 3). More specifically, we aim to predict a, b and z by hydroclimatic conditions before and during the event represented by the medians of DNT_{30}, different temporal aggregations of AI, T and Q. Again, we rely on Spearman's rank correlation to characterize and quantify the relationships more independent of their shape. Intercept z as well as coefficient b (related to Q_b) does not show any correlation at p<0.001. Model coefficient a shows good correlations (p<0.01) with T_{15}, T_{30} and Q_{30}, AI_{60} and DNT_{30} for all models. But median values of DNT_{30} and AI_{60} are the only variables
15 which showed highly significant correlations (p<0.001) with parameter a (related to Q_{hf}) for C_{DOC} as well as for the quality metrics models. Strongest increase in C_{DOC} within an event (high a) occurs when AI_{60} is low and DNT_{30} is high which translates into events during warm and dry low flow situations. On the other hand, during cold and wet high flow periods (AI_{60} and Q_b high, DNT_{30} low) large events (high Q_{hf}) produce a smaller increase of C_{DOC}. This situation typically occurs during winter.

Based on the highest r_s values in the correlation analysis for the event scale (Table 3), we selected DNT_{30} and AI_{60} as variables to explain seasonal variations in regression coefficient a. The results were used to build a regression model for all available data of C_{DOC}, $SUVA_{254}$ and $S_{275\text{-}295}$. Therefore, predictors Q_{hf} and Q_b of the event-scale models were extended by
25 seasonal-scale AI_{60} and DNT_{30} and valid interactions (VIF < 10, Eq. (1)) log(Q_{hf})×Q_b, AI_{60}×DNT_{30} and DNT_{30}×Q_b, which can account for the temporal changes in the relationships of C_{DOC} and DOC quality with discharge. Note that we, again, rely on power law behavior of C_{DOC} but logarithmic (semi-log) behavior for $SUVA_{254}$ and $S_{275\text{-}295}$ (above):

$$Y = z + a \, \log(Q_{hf}) + b \, Q_b + c \, AI_{60} + d \, DNT_{30} + i \tag{3}$$

where Y represents one of the three dependent variables log(C_{DOC}), $SUVA_{254}$ and $S_{275\text{-}295}$. a, b, c, d are regression coefficients,
30 z is the intercept. i indicates valid interaction terms (VIF < 10, Eq. (1)) log(Q_{hf})×Q_b, AI_{60}×DNT_{30} and DNT_{30}×Q_b.

The results of the modelling are depicted in Table 4 and Fig. 4. A basic overview of all regression parameters and model statistics is given in Table S1. The C_{DOC} model performs best, explaining most of the overall variance ($R^2 = 0.72 \pm 0.04$ five-

fold cross-validation prediction error), compared to the mean R² of 0.84 for modeling single events only. $SUVA_{254}$ and $S_{275-295}$ models explain similar parts (0.64 ± 0.2 and 0.65 ± 0.0) of the overall variance compared to the mean R² for the events of 0.83 and 0.64, respectively. All models generally explain both, seasonal and event-scale variability (Fig. 4, R² see Table S2), but towards small values, residuals of the DOC quality models tend to overestimate, whereas residuals of the C_{DOC} model

5   increase with increasing concentration (Fig. S3). Still, 95% of the residuals lie within a range of 1.08 mg L^{-1} and -0.90 mg L^{-1}, ± 0.44 L m^{-1}mg-C^{-1} and ± 2.2 ×10^{-3} nm^{-1} for the C_{DOC}, $SUVA_{254}$ and $S_{275-295}$ models, respectively.

Inspection of models taking only event-scale predictors (log(Q_{hf}), Q_b and interaction) or only seasonal-scale predictors (AI_{60}, DNT_{30} plus their interaction) into account reveals that both sets of variables can explain a comparable part of the total variance (R² event scale: 0.40, 0.36, 0.47; R² seasonal scale: 0.42, 0.36, 0.48 for the C_{DOC}, $SUVA_{254}$ and $S_{275-295}$ models,

10   respectively). Yet, when only using seasonal-scale drivers (AI_{60} and DNT_{30} plus their interaction), the general trend but no event-type variability is reproduced in the model (Fig. 4). On the other hand, the discharge only model does not reproduce baseflow and peak height well during the seasons.

For the C_{DOC} and $SUVA_{254}$ model, seasonal-scale drivers AI_{60} and DNT_{30} plus their interaction $DNT_{30}{\times}AI_{60}$ and event-scale driver log(Q_{hf}) alone are the most important predictors, able to explain 68% of the total variance for C_{DOC} and 54% for

15   $SUVA_{254}$ compared to 72% and 64% of the respective complete models (Table 4). In contrast to the C_{DOC} and $SUVA_{254}$ models, the interaction of seasonal-scale drivers ($DNT_{30}{\times}AI_{60}$) barely influences the R² of the $S_{275-295}$ model, but rather DNT_{30} plus the interaction of $DNT_{30}{\times}Q_b$ and event-scale hydrological drivers log(Q_{hf}) and Q_b which alone can explain 54% of the variance compared to 65% of the complete model.

20   Interactions between AI_{60} and DNT_{30} play a crucial role in the C_{DOC} and $SUVA_{254}$ models. There is a small negative effect of increasing soil wetness during low DNT_{30} values and a small negative DNT_{30} effect for dry soils. However, if exposed to increasing AI_{60} values/ soil wetness, the effect of medium and high DNT_{30} values changes towards a positive interaction. Hence, when AI_{60} is low and DNT_{30} high, which typically occurs during the summer months (Fig. 2b) or vice versa in winter, interaction leads to the lowest mean C_{DOC} and $SUVA_{254}$ values during non-precipitation periods (Fig. S4a, b). With medium

25   AI_{60} and DNT_{30} values around autumn and spring, the interaction (Fig. S4c) has more positive influence on C_{DOC} and $SUVA_{254}$ values, resulting in higher baseflow C_{DOC} and $SUVA_{254}$ values. This interaction can thus represent the change of model coefficient a that was observed in the event analysis (Fig. 3). In comparison to the C_{DOC} and $SUVA_{254}$ models, for the $S_{275-295}$ model rather the interaction of log(Q_{hf}) with Q_b has direct influence on the time variant model coefficient a and thus more influence on the R² (Table 4).

30   There is a positive effect of increasing Q_b at low and medium log(Q_{hf}) values and a positive log(Q_{hf}) effect during low Q_b. However, the effect of log(Q_{hf}) changes towards a negative interaction if exposed to increasing Q_b so that log(Q_{hf}) barely increases $S_{275-295}$ values during high Q_b situations.

4 Discussion

The regression models for the discharge events revealed that discharge had a seasonally differing impact on DOC concentration and quality observed in the Rappbode stream (Fig. 3). We argue that C_{DOC} and DOC quality changed most distinctly with the discharge components Q_{hf} and Q_b when it is warm (in the summers, Fig. 3) because during that time the largest amounts of DOC are available to be transported from the riparian soils to the stream. Contrarily, in the winter the increase in concentration is less pronounced (low model coefficient a, Fig. 3) because there is less DOC available to be washed out due to the lower temperatures and permanent hydrological connectivity between the riparian source zone of DOC and the stream. Different hydroclimatic variables can explain this dynamic (Table 3) and thus help identifying the dominant drivers for DOC concentration and quality in the study catchments.

4.1 Hydroclimatic classification

The complete regression models in our study (section 3.2.2) implemented event-scale drivers $\log(Q_{hf})$ and Q_b as well as more seasonally driven variables AI_{60}, DNT_{30} and their interactions. Consequently, hydrological and seasonal-scale drivers are both dominant controls of DOC concentrations and quality. Seasonality of hydroclimatic variables is often referred to in the literature as an important factor for DOC export dynamics (Ågren et al., 2007; Birkel et al., 2014; Köhler et al., 2009; Seibert et al., 2009) because hydroclimatic forcing influences typical mechanistic drivers like soil wetness and temperature (Broder et al., 2017; Christ and David, 1996; Garcia-Pausas et al., 2008; Preston et al., 2011). In a multivariate regression approach Köhler et al. (2009) further accounted for hydrological connectivity in order to explain monthly and annual TOC variations. Recently, Shang et al. (2018) suggested that DOM mobilization and quality is facilitated by a combination of temperature and soil-stream hydrological connectivity. To estimate how these mechanistic drivers interact to produce the observed non-linear responses of DOC concentrations and quality in our study catchment, we can separate the observation period into three distinct hydroclimatic states, which are based on the seasonal-scale predictors of the complete regression models (Fig. 5): 1) high DNT_{30} and low AI_{60}, representing warm & dry situations mainly found in summer 2) moderate DNT_{30} and AI_{60}, representing intermediate warm and wet situations, mainly found in spring and autumn and 3) low DNT_{30} and high AI_{60}, representing cold & wet situations mainly found in winter. To synthesize our modelling results in terms of potential underlying mobilization processes, these three states were compared by looking at both event and non-event responses of DOC concentrations and quality during those states.

Daily mean C_{DOC}, $SUVA_{254}$ and $S_{275-295}$ values of 1.49 mg L^{-1}, 5 ×10^{-3} nm^{-1} and 0.68 L m^{-1} mg-C^{-1} were minimal at the end of the drought in August 2013, when baseflow levels were low, whereas values of 4.14 mg L^{-1}, 15.8 ×10^{-3} nm^{-1} and 4.05 L m^{-1}

mg-C^{-1} are measured during phases with higher baseflow levels in the cold & wet state. C_{DOC}, $SUVA_{254}$ and $S_{275-295}$ values showed the strongest increase during warm & dry situations (Fig. 5) also indicated by highest slopes of model coefficient a (event-scale models, Fig. 3). The intermediate state still pronounced increasing C_{DOC}, $SUVA_{254}$ and $S_{275-295}$ values during events, but variance and range decreased compared to summer events (Fig. 5). Changes due to events in cold & wet

5   situations were small in range and variance. Variance and mean of $S_{275-295}$ were generally lower during warm & dry situations than during intermediate and cold & wet phases. Therefore we conclude that seasonal hydroclimatic variance controls the overall variance of $S_{275-295}$, whereas C_{DOC} and $SUVA_{254}$ are driven through event type variance.

4.2 Conceptual model of DOC mobilization from the riparian zone

The relationship between AI_{60} and DNT_{30} in combination with differences in DOC concentration and quality of the three

10   states is of particular interest to support a mechanistic explanation for differing DOC export during events. Hence, these metrics can be utilized for conceptualizing DOC mobilization dynamics of seasonal-scale variations in C_{DOC} and the observed quality –discharge dependencies (Fig. 6).

15   1)   Warm & dry situations

Warm & dry situations are hydroclimatically defined by high temperatures and low mean discharge (high DNT_{30}), relatively dry soil conditions (low AI_{60}) as well as low baseflow levels, as typically found in summer when the Rappbode is fed mainly by deeper riparian groundwater. During baseflow conditions highly processed DOC enters the stream via the deeper groundwater flow paths (Broder et al., 2017). DOC in deeper groundwater usually has passed through multiple soil layers, its

20   amount and its composition has been altered by sorption and biogeochemical processes (Inamdar et al., 2011; Kaiser and Kalbitz, 2012; Shen et al., 2015). Low $S_{275-295}$ values indicate high molecular weight of DOC with a dominance of terrestrial waters (Helms et al., 2008; Spencer et al., 2012) entering the stream during that time. In contrast, Raeke et al. (2017) found higher molecular weight molecules at elevated discharge in three temperate catchments (including the one studied here). However, they used grab samples from different hydroclimatic situations and streams, thus potentially masking the event-

25   scale dynamics of DOC mobilization as revealed in the current study. But also the magnitude of instream processing and biodegradation could further influence DOC composition and hence $SUVA_{254}$ and $S_{275-295}$ measurements in stream water (Bernal et al., 2018; Hansen et al., 2016). Precipitation events can get buffered and retarded in the soils (low Q_{hf}) (state warm & dry, Fig. 6). Due to the soil type and generally high groundwater tables in our catchment, soil moisture can remain high, even when there was no rainfall for some time. Hence favorable conditions for the accumulation of DOC during non-event

30   periods exist in the subsurface due to the lack of moving water in the topsoil, where the high temperatures allow for (microbially driven) riparian DOC production and accumulation.

Precipitation water infiltrates into riparian soils and activates the accumulated shallow DOC sources. During events, higher DOC concentrations with different quality were able to override the low flow DOC signal towards a riparian zone signal,

since C_{DOC} during non-event situations was very low (Fig. 5). Respective fingerprints during events changed markedly towards higher $SUVA_{254}$ values typical for processed DOC (Hansen et al., 2016; Helms et al., 2008) and higher $S_{275-295}$ (but not as high as in cold & wet) indicating a relative increase in low molecular weight components. The measurements therefore indicate the shift from a groundwater DOC signal to the mobilization of a distinct processed riparian DOC source.

5   The capacity of the system to drain and produce discharge generally increases with the rise of the groundwater table in the riparian zone. This has been called the transmissivity feedback mechanism (Seibert et al., 2009), but also preferential flow paths could play a considerable role (Hrachowitz et al., 2016). Low Q_b values during the non-event situation indicate that major parts of the discharge increase are due to an increase in event water (Q_{hf}). We argue that the increase of C_{DOC} and change of DOC quality with discharge is due to the addition of a new, distinct DOC source, connected via transmissivity

10   feedback and preferential flow paths. The (de)activation of an additional DOC source with changes in discharge could explain the observed lower R² values in the event analysis during summer (Fig. 3). The mobilized shallow DOC distinctly changes both stream C_{DOC} and quality, overprinting the groundwater signal observed before the event. Accordingly, DOC showed the highest concentration and quality peaks and event analysis revealed the steepest C-Q_{hf} and quality-Q_{hf} relations in summer. After the event, C_{DOC} and DOC quality metrics gradually drop back to the baseflow signal.

15   2)   Intermediate state

Intermediate DNT_{30} and AI_{60} conditions are defined by moderate temperatures and discharge (medium DNT_{30}), precipitation and evapotranspiration (medium AI_{60}) which pronounces in higher baseflow levels as compared to warm & dry conditions. Strong precipitation events still translate into a distinct discharge signal (high Q_{hf}) (state intermediate, Fig. 6). Conditions for the accumulation of DOC during non-event periods are less favorable due to colder temperatures than warm & dry,

20   decreasing the riparian DOC production. During baseflow conditions some of the riparian DOC pools are already activated due to a higher groundwater table. This mixing of riparian and deeper groundwater DOC pools translates into intermediate values of concentration and quality parameters, even under non-event conditions.

In case precipitation increases discharge, the DOC signal changes both concentration and quality. This process happens faster than during the warm & dry situation, since antecedent wet conditions facilitate DOC mobilization from riparian soils.

25   Hence the temporal shift between DOC and discharge peak diminishes, resulting in higher R² values during events. There was no exhaustion of the exportable DOC by consecutive events although there is less DOC production paired with more effective export mechanisms, highlighting the large store of DOC in the comparably small riparian zone. The intermediate situation averages multiple situations (transition states in autumn and spring) and thus does not have the character and clarity of the endmembers. Similar quality signals indicate the same process and location of source zone activation in autumn 2013

30   and 2014. However, concentration peaks developed differently, suggesting that the conditions for antecedent DOC storage and export during preceding phases were different. Intermediate DNT_{30} and AI_{60} levels and hence only little mobilization and storage limitations in spring 2014 translated into pronounced DOC export during events. However, DOC quality, especially $S_{275-295}$ barely changed during these events. Elevated temperatures during this period cause a warming of riparian topsoil,

which are rich in organic matter, and hence an increase in biological processing and DOC production. Declining, still high baseflow levels and soil moisture lead to increased DOC production and export during these events.

3) Cold & wet situations

Cold & wet situations, typically found in winter, are defined by low temperatures and high mean discharge (low DNT_{30}),
humid conditions (high AI_{60}) as well as high baseflow levels (state cold & wet, Fig. 6). Generally low C_{DOC} values indicate a limited availability of DOC in the riparian zone in comparison to the generated runoff. Unfavorable conditions for the accumulation of DOC during non-event periods exist in the topsoil, where the low temperature impairs riparian DOC production. Accordingly, low $SUVA_{254}$ and high $S_{275-295}$ values were observed during that period, indicating relatively higher amount of low molecular weight compounds due to reduced DOC processing. Furthermore, high base flow levels lead to a
good hydrological connectivity of DOC sources to the stream. In addition, this dominant hydrological state could be able to leach differing DOC from the riparian zone by shifts in physicochemical equilibria (Shen et al., 2015) thereby forming the corresponding quality.

Precipitation events result in small, sometimes even negative slopes of the C_{DOC} and quality-Q_{hf} relationships indicating some dilution. Dilution due to the impermeability of the frozen soil surface (Laudon et al., 2007), but also limitations due to
the depletion of exportable DOC sources due to low production of DOC at low temperatures could occur. Due to high Q_b levels riparian soils are presumably saturated and precipitation events lead to a rapid but minor increase in an already high stream discharge (high Q_{hf}). Also, since riparian DOC pools are already connected to the stream, there is no big change of concentration and quality detectable during events. We attribute the small shift in DOC quality and C_{DOC} during events to a shift of the distribution (hydrological connection) of DOC source areas with similar DOC quality, rather than to the
activation of new, differing DOC pools. This could also explain the high R² but low regression coefficient a of event modeling during winter and spring events for C_{DOC} and $SUVA_{254}$ models (Fig. 3): since all sources were connected already during the non-event phase, hydrological forcing did not have much impact on these DOC characteristics. In contrast to C_{DOC} and $SUVA_{254}$, R² of $S_{275-295}$ drops during the cold & wet situation, indicating a decoupling from hydrologic forcing. This finding needs further research. In general, the low variance of C_{DOC} and quality during winter indicates a steady activation of
most available source zones. High AI_{60} values in winter indicate no mobilization limitation; high baseflow levels indicate a good hydrological connectivity of the stream to riparian DOC sources. The same observations of C_{DOC} and quality interaction during winter and spring (low DOC variance in winter, still low quality variance but strong C_{DOC} fluctuations in spring) were made in 2013. But due to the lack of weather data, no further statements can be made to this time of the year (Fig. 2).

5 Conclusions

Observing DOC concentration and quality, as well as discharge and seasonal dynamics, at high frequency allows a more in-depth evaluation of DOC export mechanisms because quality metrics support the interpretation of measurements of DOC

quantity by adding information about processing and mobilization and thus possibly also about the source locations in the riparian zone.

The temporal dynamics of DOC concentration and quality can be captured by a combination of hydrological event-scale drivers and hydroclimatic metrics, which define the conditions prior to the event. Model evaluation highlights the importance

5 of seasonal-scale antecedent predictors AI_{60} and DNT_{30} on DOC concentration and quality dynamics. AI_{60} describes the potential for mobilizing DOC in riparian soils, whereas DNT_{30} describes the changes in DOC storage by looking at the relationship of DOC production and prior mean export from riparian soils. Hence, the relationship of AI_{60} and DNT_{30} describes DOC depletion or accumulation in riparian soils. Evaluation of seasonal-scale drivers AI_{60} and DNT_{30} suggested that cold & wet situations are not mobilization limited (high mobilization potential due to wet soils and high baseflow levels)

10 but limited in production and processing (due to low temperatures). High hydrological connectivity therefore translates into low C_{DOC} and a depletion of the pools of freshly processed DOC. Events do not change the quality signature of the DOC in the stream, since all riparian DOC sources were already connected to the stream before. In contrast, we interpret warm & dry conditions as mobilization-limited situations (dryer soils, low baseflow levels) at high DOC production rates (high temperatures) and low hydrological connectivity, which leads to an accumulation of DOC in the upper soil layers of the

15 riparian zone during non-event situations and export of highly processed DOC from deeper soil layers with baseflow contributions to the stream. DOC composition varies the most during such warmer dry periods. During non-event conditions, the system is transport limited and decomposition of organic material is most pronounced.

Events change the DOC-quality signature in the stream water by adding freshly processed DOC from upper riparian DOC sources to the older more intensely processed DOC from the underlying base flow signature. The relationship of AI_{60} and

20 DNT_{30} to C_{DOC} and DOC quality thus is of particular interest for conceptualizing our understanding of DOC mobilization dynamics in concentration/quality – discharge dependencies since it facilitates a mechanistic interpretation of DOC export from riparian zones.

Yet, it remains unclear which explicit mechanisms in the riparian zone are responsible for the measured and conceptualized DOC dynamics in the Rappbode stream. Our interpretation is based on the integrated signal of DOC concentration and

25 quality measured in the stream. Further research is necessary to identify the explicit spatio-temporal mobilization patterns as well as molecular markers that can be used to trace DOC from riparian source zones into the stream in order to fully understand DOC mobilization in the riparian zone.

The findings reported and analyzed here provide a mechanistic explanation of the seasonally changing characteristics of DOC-discharge relationships and therefore can be utilized to infer the spatio-temporal dynamics of the DOC origin in

30 riparian zones from the DOC dynamics of headwater streams.

This study helps to understand DOC concentration and quality dynamics in temperate head water catchments. Furthermore, the study facilitates the application of strategies for drinking water purification. In addition, this study highlights the dependency of DOC export on hydroclimatic factors. Potential impacts of climate change on the amount and quality of exported DOC are therefore likely and should be further investigated.

Data availability. All data sets used in this synthesis are publicly available via the link: https://doi.org/10.4211/hs.e0e6fbc0571149b79b1e75fa44d5c4ab.

5 *Author contributions*. JF, OL, AM and GdR planned and designed the research. MO carried out parts of the field work and conducted a first version of data processing and analysis. BW did the statistical analysis and wrote the paper with contributions from all co-authors.

Competing interests. The authors declare that they have no conflict of interest.

Acknowledgements. Acquisition of data was financially supported by the Federal Ministry of Education and Research Germany [grant number BMBF, 02WT1290A]. Special thanks to Toralf Keller for excellent and steady field work as well as to Wolf von Tümpling for the support in the laboratory.

References

15 Ågren, A., Berggren, M., Laudon, H., and Jansson, M.: Terrestrial export of highly bioavailable carbon from small boreal catchments in spring floods, Freshwater Biology, 53, 964-972, doi:10.1111/j.1365-2427.2008.01955.x, 2008.

Ågren, A., Jansson, M., Ivarsson, H., Bishop, K., and Seibert, J.: Seasonal and runoff-related changes in total organic carbon concentrations in the River Öre, Northern Sweden, Aquatic Sciences, 70, 21-29, doi:10.1007/s00027-007-0943-9, 2007.

Alarcon-Herrera, M. T., Bewtra, J. K., and Biswas, N.: Seasonal variations in humic substances and their reduction through 20 water treatment processes, Canadian Journal of Civil Engineering, 21, 173-179, doi:10.1139/l94-020, 1994.

Allen, R. G., Pereira, L. S., Raes, D., and Smith, M.: Crop evapotranspiration. Guidelines for computing crop water requirements. , FAO, Rome, 1998.

Barrow, C. J.: World atlas of desertification (United nations environment programme), edited by N. Middleton and D. S. G. Thomas. Edward Arnold Land Degradation & Development, 3, 249-249, doi:10.1002/ldr.3400030407, 1992.

25 Battin, T. J., Luyssaert, S., Kaplan, L. A., Aufdenkampe, A. K., Richter, A., and Tranvik, L. J.: The boundless carbon cycle, Nature Geoscience, 2, 598, doi:10.1038/ngeo618, 2009.

Berggren, M. and del Giorgio, P. A.: Distinct patterns of microbial metabolism associated to riverine dissolved organic carbon of different source and quality, Journal of Geophysical Research: Biogeosciences, 120, 989-999, doi:10.1002/2015jg002963, 2015.

30 Bernal, S., Lupon, A., Catalán, N., Castelar, S., and Martí, E.: Decoupling of dissolved organic matter patterns between stream and riparian groundwater in a headwater forested catchment, Hydrology and Earth System Sciences, 22, 1897-1910, doi:10.5194/hess-22-1897-2018, 2018.

Birkel, C., Soulsby, C., and Tetzlaff, D.: Integrating parsimonious models of hydrological connectivity and soil biogeochemistry to simulate stream DOC dynamics, J Geophys Res-Biogeo, 119, 1030-1047, doi:10.1002/2013jg002551, 35 2014.

Bishop, K. H., Grip, H., and O'Neill, A.: The origins of acid runoff in a hillslope during storm events, Journal of Hydrology, 116, 35-61, doi:10.1016/0022-1694(90)90114-d, 1990.

Blaen, P. J., Khamis, K., Lloyd, C., Comer-Warner, S., Ciocca, F., Thomas, R. M., MacKenzie, A. R., and Krause, S.: High-frequency monitoring of catchment nutrient exports reveals highly variable storm event responses and dynamic source zone 40 activation, Journal of Geophysical Research: Biogeosciences, 122, 2265-2281, doi:10.1002/2017jg003904, 2017.

Botter, G., Basso, S., Rodriguez-Iturbe, I., and Rinaldo, A.: Resilience of river flow regimes, Proceedings of the National Academy of Sciences, 110, 12925-12930, doi:10.1073/pnas.1311920110, 2013.

Broder, T., Knorr, K. H., and Biester, H.: Changes in dissolved organic matter quality in a peatland and forest headwater stream as a function of seasonality and hydrologic conditions, Hydrol. Earth Syst. Sci., 21, 2035-2051, doi:10.5194/hess-21-2035-2017, 2017.

Buffam, I., Galloway, J. N., Blum, L. K., and McGlathery, K. J.: A stormflow/baseflow comparison of dissolved organic matter concentrations and bioavailability in an Appalachian stream, Biogeochemistry, 53, 269-306, doi:10.1023/a:1010643432253, 2001.

Chantigny, M. H.: Dissolved and water-extractable organic matter in soils: a review on the influence of land use and management practices, Geoderma, 113, 357-380, doi:https://doi.org/10.1016/S0016-7061(02)00370-1, 2003.

Christ, M. J. and David, M. B.: Temperature and moisture effects on the production of dissolved organic carbon in a Spodosol, Soil Biology and Biochemistry, 28, 1191-1199, doi:https://doi.org/10.1016/0038-0717(96)00120-4, 1996.

Cole, J. J., Prairie, Y. T., Caraco, N. F., McDowell, W. H., Tranvik, L. J., Striegl, R. G., Duarte, C. M., Kortelainen, P., Downing, J. A., Middelburg, J. J., and Melack, J.: Plumbing the Global Carbon Cycle: Integrating Inland Waters into the Terrestrial Carbon Budget, Ecosystems, 10, 172-185, doi:10.1007/s10021-006-9013-8, 2007.

Creed, I. F., McKnight, D. M., Pellerin, B., Green, M. B., Bergamaschi, B., Aiken, G. R., Burns, D. A., Findlay, S. E. G., Shanley, J. B., Striegl, R. G., Aulenbach, B. T., Clow, D. W., Laudon, H., McGlynn, B. L., McGuire, K. J., Smith, R. A., and Stackpoole, S. M.: The river as a chemostat: fresh perspectives on dissolved organic matter flowing down the river continuum, Canadian Journal of Fisheries and Aquatic Sciences, 72, 1272-1285, doi:10.1139/cjfas-2014-0400, 2015.

Eran, H., N., G. M., and L., J. S.: Changes in the character of stream water dissolved organic carbon during flushing in three small watersheds, Oregon, Journal of Geophysical Research: Biogeosciences, 111, doi:10.1029/2005JG000082, 2006.

Etheridge, J. R., Birgand, F., Osborne, J. A., Osburn, C. L., Burchell, M. R., and Irving, J.: Using in situ ultraviolet-visual spectroscopy to measure nitrogen, carbon, phosphorus, and suspended solids concentrations at a high frequency in a brackish tidal marsh, Limnology and Oceanography: Methods, 12, 10-22, doi:10.4319/lom.2014.12.10, 2014.

Evans, C. D., Monteith, D. T., and Cooper, D. M.: Long-term increases in surface water dissolved organic carbon: observations, possible causes and environmental impacts, Environ Pollut, 137, 55-71, doi:10.1016/j.envpol.2004.12.031, 2005.

Fox, J. and Weisberg, S.: An {R} Companion to Applied Regression. Sage, 2011.

Freeman, C., Evans, C. D., Monteith, D. T., Reynolds, B., and Fenner, N.: Export of organic carbon from peat soils, Nature, 412, 785, doi:10.1038/35090628, 2001.

Garcia-Pausas, J., Casals, P., Camarero, L., Huguet, C., Thompson, R., Sebastià, M.-T., and Romanyà, J.: Factors regulating carbon mineralization in the surface and subsurface soils of Pyrenean mountain grasslands, Soil Biology and Biochemistry, 40, 2803-2810, doi:https://doi.org/10.1016/j.soilbio.2008.08.001, 2008.

Guarch-Ribot, A. and Butturini, A.: Hydrological conditions regulate dissolved organic matter quality in an intermittent headwater stream. From drought to storm analysis, Science of The Total Environment, 571, 1358-1369, doi:https://doi.org/10.1016/j.scitotenv.2016.07.060, 2016.

Gustard, A. and Demuth, S.: Manual on Low-flow Estimation and Prediction, World Meteorological Organization (WMO), 2009.

Hansen, A. M., Kraus, T. E. C., Pellerin, B. A., Fleck, J. A., Downing, B. D., and Bergamaschi, B. A.: Optical properties of dissolved organic matter (DOM): Effects of biological and photolytic degradation, Limnology and Oceanography, 61, 1015-1032, doi:10.1002/lno.10270, 2016.

Helms, J. R., Stubbins, A., Ritchie, J. D., Minor, E. C., Kieber, D. J., and Mopper, K.: Absorption spectral slopes and slope ratios as indicators of molecular weight, source, and photobleaching of chromophoric dissolved organic matter, Limnology and Oceanography, 53, 955-969, doi:10.4319/lo.2008.53.3.0955, 2008.

Herzsprung, P., von Tumpling, W., Hertkorn, N., Harir, M., Buttner, O., Bravidor, J., Friese, K., and Schmitt-Kopplin, P.: Variations of DOM quality in inflows of a drinking water reservoir: linking of van Krevelen diagrams with EEMF spectra by rank correlation, Environ Sci Technol, 46, 5511-5518, doi:10.1021/es300345c, 2012.

Hood, E., Gooseff, M. N., and Johnson, S. L.: Changes in the character of stream water dissolved organic carbon during flushing in three small watersheds, Oregon, J Geophys Res-Biogeo, 111, doi:Artn G01007

10.1029/2005jg000082, 2006.

Hope, D., Billett, M. F., and Cresser, M. S.: A review of the export of carbon in river water: Fluxes and processes, Environmental Pollution, 84, 301-324, doi:10.1016/0269-7491(94)90142-2, 1994.

Hrachowitz, M., Benettin, P., van Breukelen, B. M., Fovet, O., Howden, N. J. K., Ruiz, L., van der Velde, Y., and Wade, A. J.: Transit times-the link between hydrology and water quality at the catchment scale, Wiley Interdisciplinary Reviews: Water, 3, 629-657, doi:10.1002/wat2.1155, 2016.

Hruška, J., Krám, P., McDowell, W. H., and Oulehle, F.: Increased Dissolved Organic Carbon (DOC) in Central European Streams is Driven by Reductions in Ionic Strength Rather than Climate Change or Decreasing Acidity, Environmental Science & Technology, 43, 4320-4326, doi:10.1021/es803645w, 2009.

Hutchins, R. H. S., Aukes, P., Schiff, S. L., Dittmar, T., Prairie, Y. T., and del Giorgio, P. A.: The Optical, Chemical, and Molecular Dissolved Organic Matter Succession Along a Boreal Soil-Stream-River Continuum, Journal of Geophysical Research: Biogeosciences, 122, 2892-2908, doi:10.1002/2017jg004094, 2017.

Inamdar, S., Finger, N., Singh, S., Mitchell, M., Levia, D., Bais, H., Scott, D., and McHale, P.: Dissolved organic matter (DOM) concentration and quality in a forested mid-Atlantic watershed, USA, Biogeochemistry, 108, 55-76, doi:10.1007/s10533-011-9572-4, 2011.

Jawitz, J. W. and Mitchell, J.: Temporal inequality in catchment discharge and solute export, Water Resources Research, 47, doi:10.1029/2010WR010197, 2011.

Kaiser, K. and Kalbitz, K.: Cycling downwards – dissolved organic matter in soils, Soil Biology and Biochemistry, 52, 29-32, doi:https://doi.org/10.1016/j.soilbio.2012.04.002, 2012.

Koffler, D., Gauster, T., and Laaha, G.: lfstat: Calculation of Low Flow Statistics for Daily Stream Flow Data. R package version 0.9.4, 2016. 2016.

Köhler, S. J., Buffam, I., Laudon, H., and Bishop, K. H.: Climate's control of intra-annual and interannual variability of total organic carbon concentration and flux in two contrasting boreal landscape elements, Journal of Geophysical Research, 113, doi:10.1029/2007jg000629, 2008.

Köhler, S. J., Buffam, I., Seibert, J., Bishop, K. H., and Laudon, H.: Dynamics of stream water TOC concentrations in a boreal headwater catchment: Controlling factors and implications for climate scenarios, Journal of Hydrology, 373, 44-56, doi:10.1016/j.jhydrol.2009.04.012, 2009.

Kottek, M., Grieser, J., Beck, C., Rudolf, B., and Rubel, F.: World Map of the Köppen-Geiger climate classification updated, Meteorologische Zeitschrift, 15, 259-263, doi:10.1127/0941-2948/2006/0130, 2006.

Laudon, H., Buttle, J., Carey, S. K., McDonnell, J., McGuire, K., Seibert, J., Shanley, J., Soulsby, C., and Tetzlaff, D.: Cross-regional prediction of long-term trajectory of stream water DOC response to climate change, Geophysical Research Letters, 39, n/a-n/a, doi:10.1029/2012gl053033, 2012.

Laudon, H., Sjöblom, V., Buffam, I., Seibert, J., and Mörth, M.: The role of catchment scale and landscape characteristics for runoff generation of boreal streams, Journal of Hydrology, 344, 198-209, doi:https://doi.org/10.1016/j.jhydrol.2007.07.010, 2007.

Ledesma, J. L., Grabs, T., Bishop, K. H., Schiff, S. L., and Kohler, S. J.: Potential for long-term transfer of dissolved organic carbon from riparian zones to streams in boreal catchments, Glob Chang Biol, 21, 2963-2979, doi:10.1111/gcb.12872, 2015.

Ledesma, J. L. J., Kothawala, D. N., Bastviken, P., Maehder, S., Grabs, T., and Futter, M. N.: Stream Dissolved Organic Matter Composition Reflects the Riparian Zone, Not Upslope Soils in Boreal Forest Headwaters, Water Resources Research, 54, 3896-3912, doi:10.1029/2017WR021793, 2018.

Lepisto, A., Futter, M. N., and Kortelainen, P.: Almost 50 years of monitoring shows that climate, not forestry, controls long-term organic carbon fluxes in a large boreal watershed, Glob Chang Biol, 20, 1225-1237, doi:10.1111/gcb.12491, 2014.

Marquardt, D. W.: Generalized Inverses, Ridge Regression, Biased Linear Estimation, and Nonlinear Estimation, Technometrics, 12, 591-612, doi:10.2307/1267205, 1970.

Menard, S.: Applied logistic regression analysis, SAGE publications, 2001.

Mevik, B.-H. and Wehrens, R.: TheplsPackage: Principal Component and Partial Least Squares Regression inR, Journal of Statistical Software, 18, doi:10.18637/jss.v018.i02, 2007.

Moatar, F., Abbott, B. W., Minaudo, C., Curie, F., and Pinay, G.: Elemental properties, hydrology, and biology interact to shape concentration-discharge curves for carbon, nutrients, sediment, and major ions, Water Resources Research, 53, 1270-1287, doi:10.1002/2016wr019635, 2017.

Monteith, D. T., Stoddard, J. L., Evans, C. D., de Wit, H. A., Forsius, M., Hogasen, T., Wilander, A., Skjelkvale, B. L., Jeffries, D. S., Vuorenmaa, J., Keller, B., Kopacek, J., and Vesely, J.: Dissolved organic carbon trends resulting from changes in atmospheric deposition chemistry, Nature, 450, 537-540, doi:10.1038/nature06316, 2007.

Mueller, C., Zink, M., Samaniego, L., Krieg, R., Merz, R., Rode, M., and Knöller, K.: Discharge Driven Nitrogen Dynamics
5   in a Mesoscale River Basin As Constrained by Stable Isotope Patterns, Environmental Science & Technology, 50, 9187-9196, doi:10.1021/acs.est.6b01057, 2016.

Musolff, A., Fleckenstein, J. H., Opitz, M., Büttner, O., Kumar, R., and Tittel, J.: Spatio-temporal controls of dissolved organic carbon stream water concentrations, Journal of Hydrology, doi: https://doi.org/10.1016/j.jhydrol.2018.09.011, 2018. doi:https://doi.org/10.1016/j.jhydrol.2018.09.011, 2018.

10   Musolff, A., Schmidt, C., Selle, B., and Fleckenstein, J. H.: Catchment controls on solute export, Advances in Water Resources, 86, 133-146, doi:https://doi.org/10.1016/j.advwatres.2015.09.026, 2015.

Musolff, A., Selle, B., Büttner, O., Opitz, M., and Tittel, J.: Unexpected release of phosphate and organic carbon to streams linked to declining nitrogen depositions, Global Change Biology, 23, 1891-1901, doi:10.1111/gcb.13498, 2017.

Preston, M. D., Eimers, M. C., and Watmough, S. A.: Effect of moisture and temperature variation on DOC release from a
15   peatland: Conflicting results from laboratory, field and historical data analysis, Science of The Total Environment, 409, 1235-1242, doi:https://doi.org/10.1016/j.scitotenv.2010.12.027, 2011.

R-Core-Team: R: A Language and Environment for Statistical Computing. Computing, R. F. f. S. (Ed.), 2017.

Raeke, J., Lechtenfeld, O. J., Tittel, J., Oosterwoud, M. R., Bornmann, K., and Reemtsma, T.: Linking the mobilization of dissolved organic matter in catchments and its removal in drinking water treatment to its molecular characteristics, Water
20   Res, 113, 149-159, doi:10.1016/j.watres.2017.01.066, 2017.

Rode, M., Wade, A. J., Cohen, M. J., Hensley, R. T., Bowes, M. J., Kirchner, J. W., Arhonditsis, G. B., Jordan, P., Kronvang, B., Halliday, S. J., Skeffington, R. A., Rozemeijer, J. C., Aubert, A. H., Rinke, K., and Jomaa, S.: Sensors in the Stream: The High-Frequency Wave of the Present, Environ Sci Technol, 50, 10297-10307, doi:10.1021/acs.est.6b02155, 2016.

25   Rodríguez-Iturbe, I., Ijjász-Vásquez, E. J., Bras, R. L., and Tarboton, D. G.: Power law distributions of discharge mass and energy in river basins, Water Resources Research, 28, 1089-1093, doi:10.1029/91WR03033, 1992.

Roth, V.-N., Dittmar, T., Gaupp, R., and Gleixner, G.: Latitude and pH driven trends in the molecular composition of DOM across a north south transect along the Yenisei River, Geochimica et Cosmochimica Acta, 123, 93-105, doi:10.1016/j.gca.2013.09.002, 2013.

30   Roth, V. N., Dittmar, T., Gaupp, R., and Gleixner, G.: The molecular composition of dissolved organic matter in forest soils as a function of pH and temperature, PLoS One, 10, e0119188, doi:10.1371/journal.pone.0119188, 2015.

Samaniego, L., Kumar, R., and Attinger, S.: Multiscale parameter regionalization of a grid-based hydrologic model at the mesoscale, Water Resources Research, 46, doi:10.1029/2008wr007327, 2010.

Sanderman, J., Lohse, K. A., Baldock, J. A., and Amundson, R.: Linking soils and streams: Sources and chemistry of
35   dissolved organic matter in a small coastal watershed, Water Resources Research, 45, doi:10.1029/2008wr006977, 2009.

Seibert, J., Grabs, T., Köhler, S., Laudon, H., Winterdahl, M., and Bishop, K.: Linking soil-and stream-water chemistry based on a Riparian Flow-Concentration Integration Model, Hydrology and earth system sciences, 13, 2287-2297, 2009.

Shang, P., Lu, Y., Du, Y., Jaffé, R., Findlay, R. H., and Wynn, A.: Climatic and watershed controls of dissolved organic matter variation in streams across a gradient of agricultural land use, Science of The Total Environment, 612, 1442-1453,
40   doi:https://doi.org/10.1016/j.scitotenv.2017.08.322, 2018.

Sharp, E. L., Parsons, S. A., and Jefferson, B.: The impact of seasonal variations in DOC arising from a moorland peat catchment on coagulation with iron and aluminium salts, Environmental Pollution, 140, 436-443, doi:https://doi.org/10.1016/j.envpol.2005.08.001, 2006.

Shen, Y., Chapelle, F. H., Strom, E. W., and Benner, R.: Origins and bioavailability of dissolved organic matter in
45   groundwater, Biogeochemistry, 122, 61-78, doi:10.1007/s10533-014-0029-4, 2015.

Spencer, R. G. M., Butler, K. D., and Aiken, G. R.: Dissolved organic carbon and chromophoric dissolved organic matter properties of rivers in the USA, Journal of Geophysical Research: Biogeosciences, 117, n/a-n/a, doi:10.1029/2011jg001928, 2012.

Stewart, A. and Wetzel, R.: Dissolved humic materials: Photodegradation, sediment effects, and reactivity with phosphate
50   and calcium carbonate precipitation, Arch. Hydrobiol, 92, 265-286, 1981.

Strohmeier, S., Knorr, K. H., Reichert, M., Frei, S., Fleckenstein, J. H., Peiffer, S., and Matzner, E.: Concentrations and fluxes of dissolved organic carbon in runoff from a forested catchment: insights from high frequency measurements, Biogeosciences, 10, 905-916, doi:10.5194/bg-10-905-2013, 2013.

Vaughan, M. C. H., Bowden, W. B., Shanley, J. B., Vermilyea, A., Sleeper, R., Gold, A. J., Pradhanang, S. M., Inamdar, S. P., Levia, D. F., Andres, A. S., Birgand, F., and Schroth, A. W.: High-frequency dissolved organic carbon and nitrate measurements reveal differences in storm hysteresis and loading in relation to land cover and seasonality, Water Resources Research, 53, 5345-5363, doi:10.1002/2017wr020491, 2017.

Vik, E. A. and Eikebrokk, B.: Coagulation Process for Removal of Humic Substances from Drinking Water, 219, 385-408, doi:10.1021/ba-1988-0219.ch024, 1988.

Weishaar, J. L., Aiken, G. R., Bergamaschi, B. A., Fram, M. S., Fujii, R., and Mopper, K.: Evaluation of Specific Ultraviolet Absorbance as an Indicator of the Chemical Composition and Reactivity of Dissolved Organic Carbon, Environmental Science & Technology, 37, 4702-4708, doi:10.1021/es030360x, 2003.

Wollschläger, U., Attinger, S., Borchardt, D., Brauns, M., Cuntz, M., Dietrich, P., Fleckenstein, J. H., Friese, K., Friesen, J., Harpke, A., Hildebrandt, A., Jäckel, G., Kamjunke, N., Knöller, K., Kögler, S., Kolditz, O., Krieg, R., Kumar, R., Lausch, A., Liess, M., Marx, A., Merz, R., Mueller, C., Musolff, A., Norf, H., Oswald, S. E., Rebmann, C., Reinstorf, F., Rode, M., Rink, K., Rinke, K., Samaniego, L., Vieweg, M., Vogel, H.-J., Weitere, M., Werban, U., Zink, M., and Zacharias, S.: The Bode hydrological observatory: a platform for integrated, interdisciplinary hydro-ecological research within the TERENO Harz/Central German Lowland Observatory, Environmental Earth Sciences, 76, 29, doi:10.1007/s12665-016-6327-5, 2016.
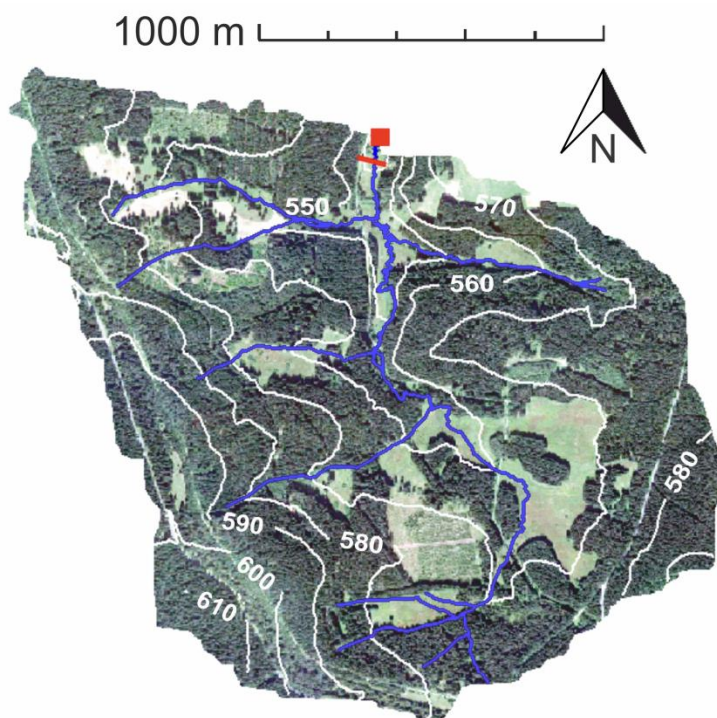
Fig. 1: Topography of the Rappbode catchment with the UV-Vis and discharge measurements at the outlet (red square). Transect for soil samples indicated by red line.
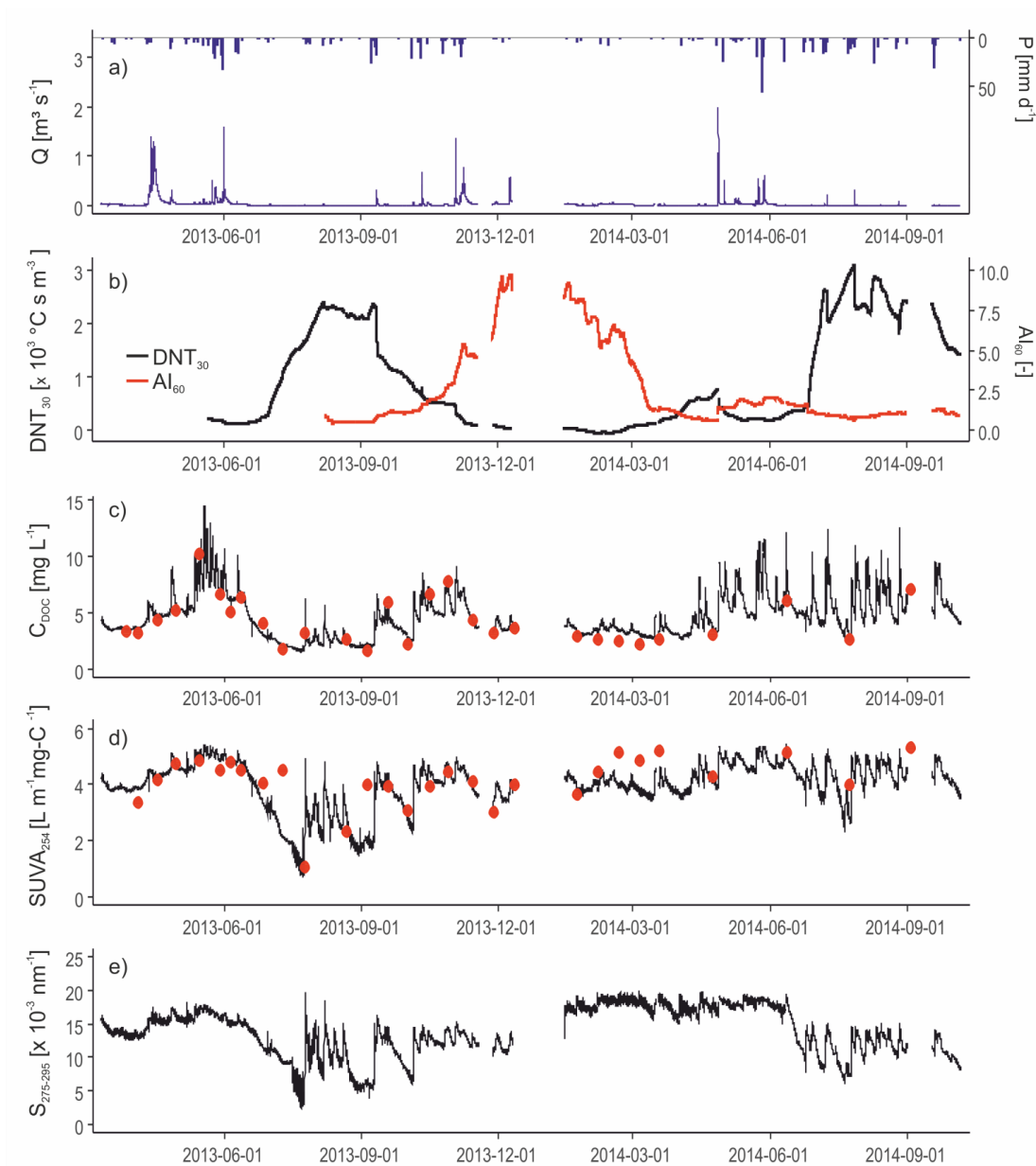
Fig. 2: (a) Precipitation and discharge, **(b)** antecedent hydro meteorological conditions, **(c)** C_{DOC}, **(d)** $SUVA_{254}$ and **(e)** $S_{275-295}$ over the entire measurement period. C_{DOC} in **(c)** was fitted with PLSR to the measured grab samples (red dots). Grab samples (red dots) in the $SUVA_{254}$ values **(d)** were just used for validation.
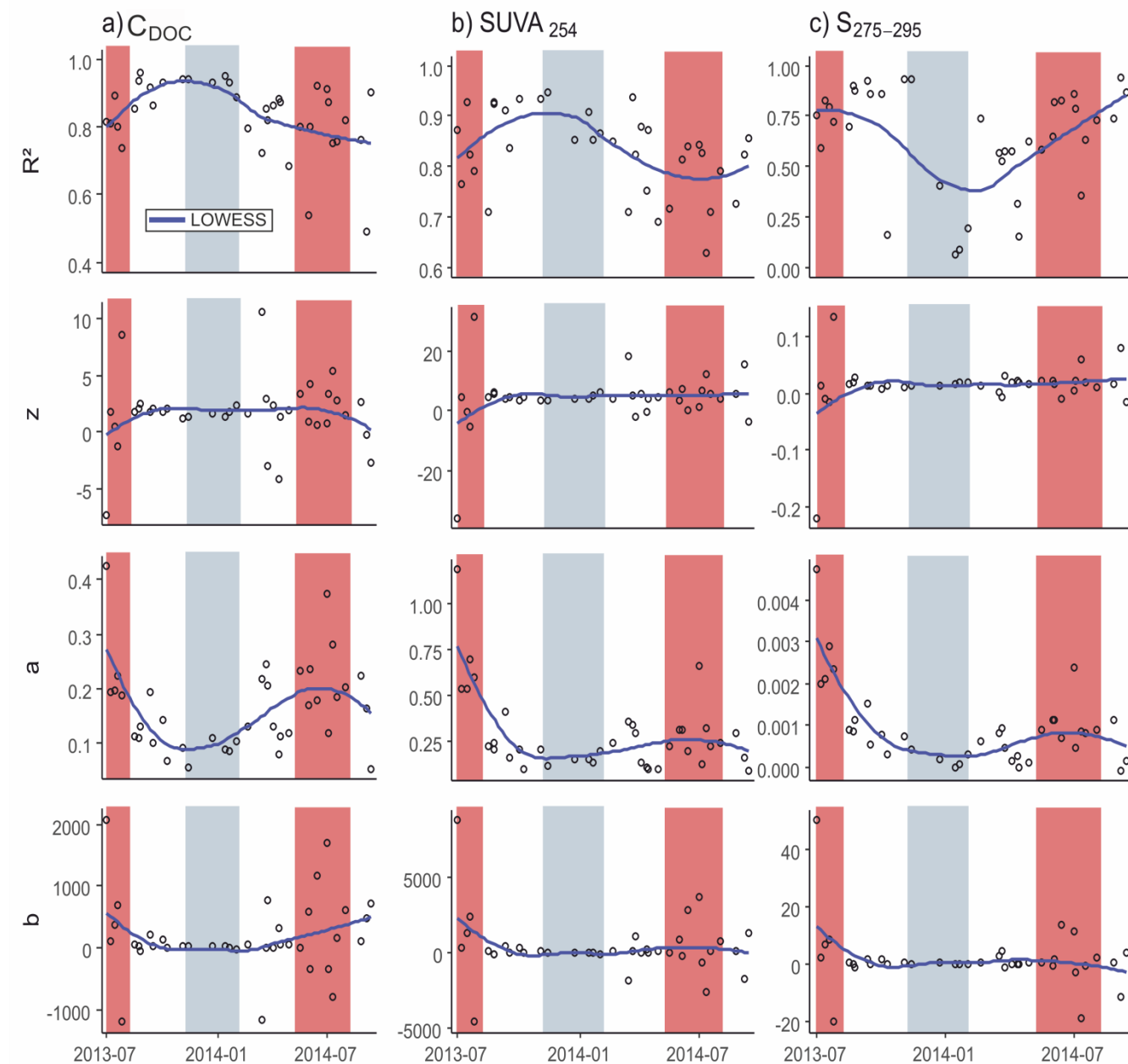
Fig. 3: R², intercept z and regression coefficients a and b of the model predictors $\log(Q_{hf})$ and Q_b in Eq. (2) of all 38 events plotted against time. The headings in the top of the figure indicate which variable was represented by Y in Eq. (2). Blue lines indicate the locally weighted scatterplot smoothing (LOWESS), background colors indicate seasons (grey = winter, red= summer, white = autumn and spring). Note the different scales of the y-axes.
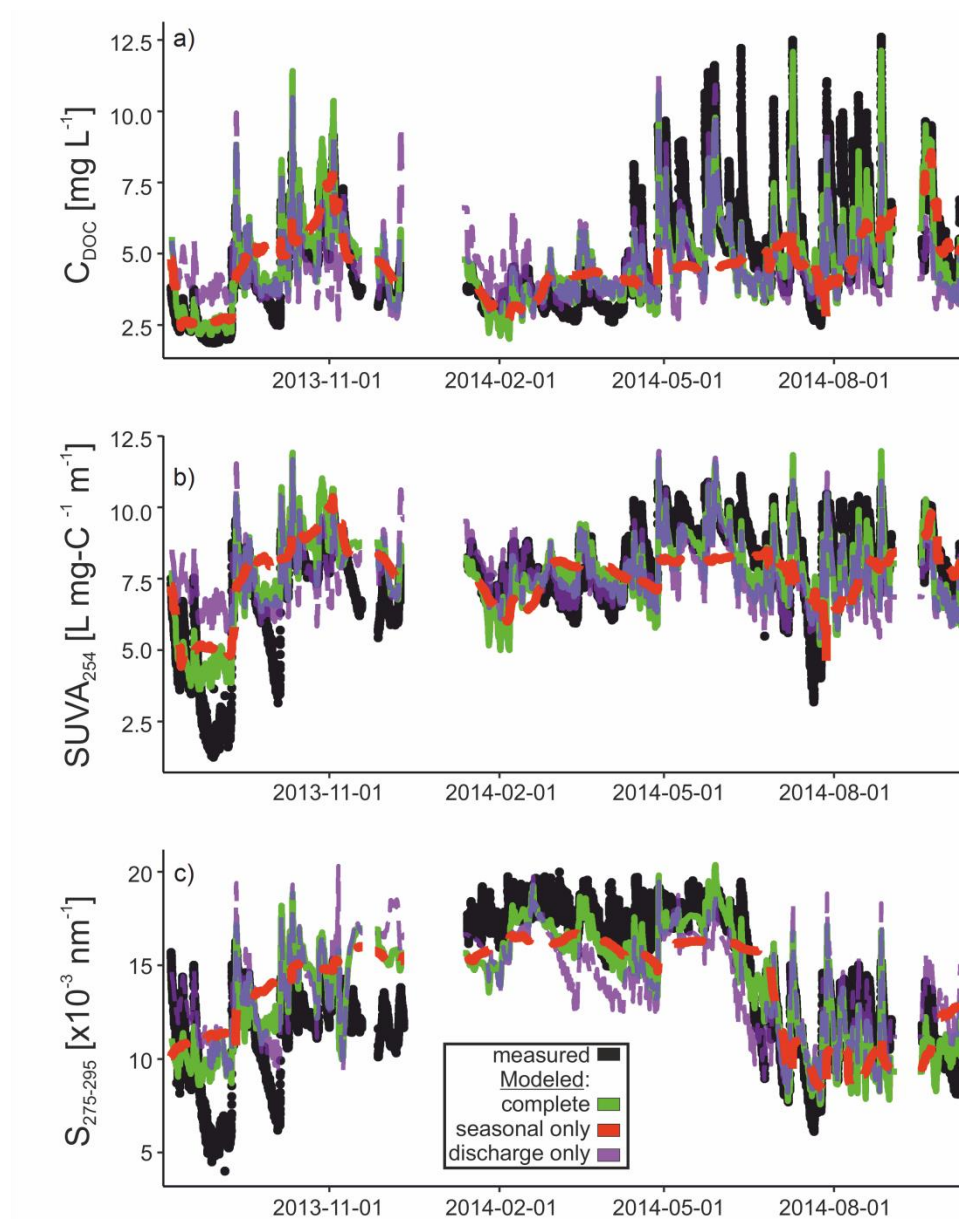
Fig. 4: Comparison between measured (black) and multiple regression models of the complete predictors (green) as given by Eq. (3), only seasonal predictors AI_{60} and DNT_{30} plus their interaction (red) and only discharge predictors $\log(Q_{hf})$ and Q_b plus their interaction (purple) for (a) C_{DOC}, (b) $SUVA_{254}$ and (c) $S_{275\text{-}295}$ values. Complete and discharge only model were smoothed (5 hourly) for better visualization.
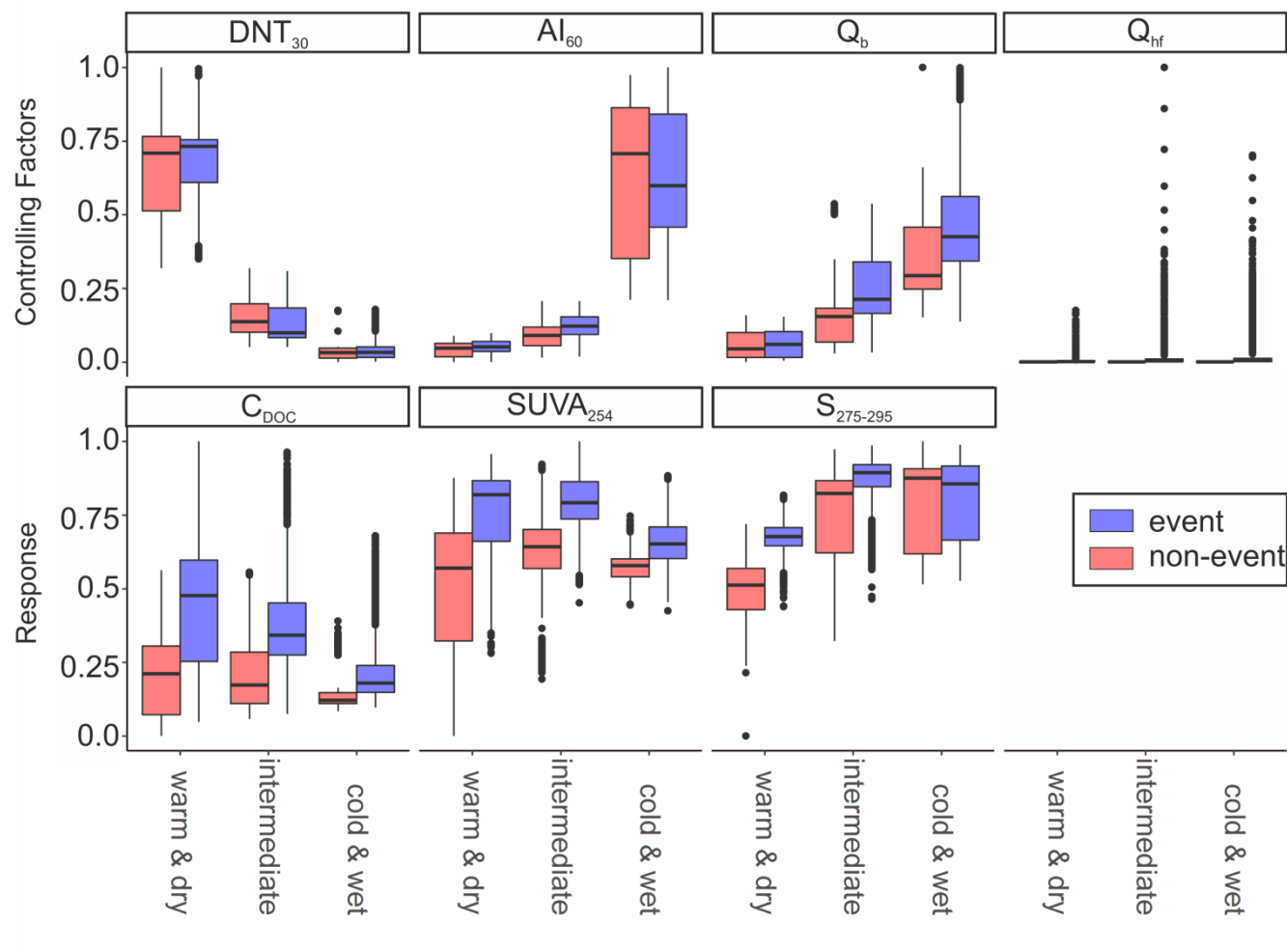
Fig. 5: Box-plots of hydroclimatic variables (controlling factors) and DOC quantity and quality metrics (response) classified into three hydroclimatic states: 1) warm & dry, 2) intermediate, 3) cold & wet. Red color indicates non-event situations, purple color event situations during the according states. Variables were rescaled for better illustration.
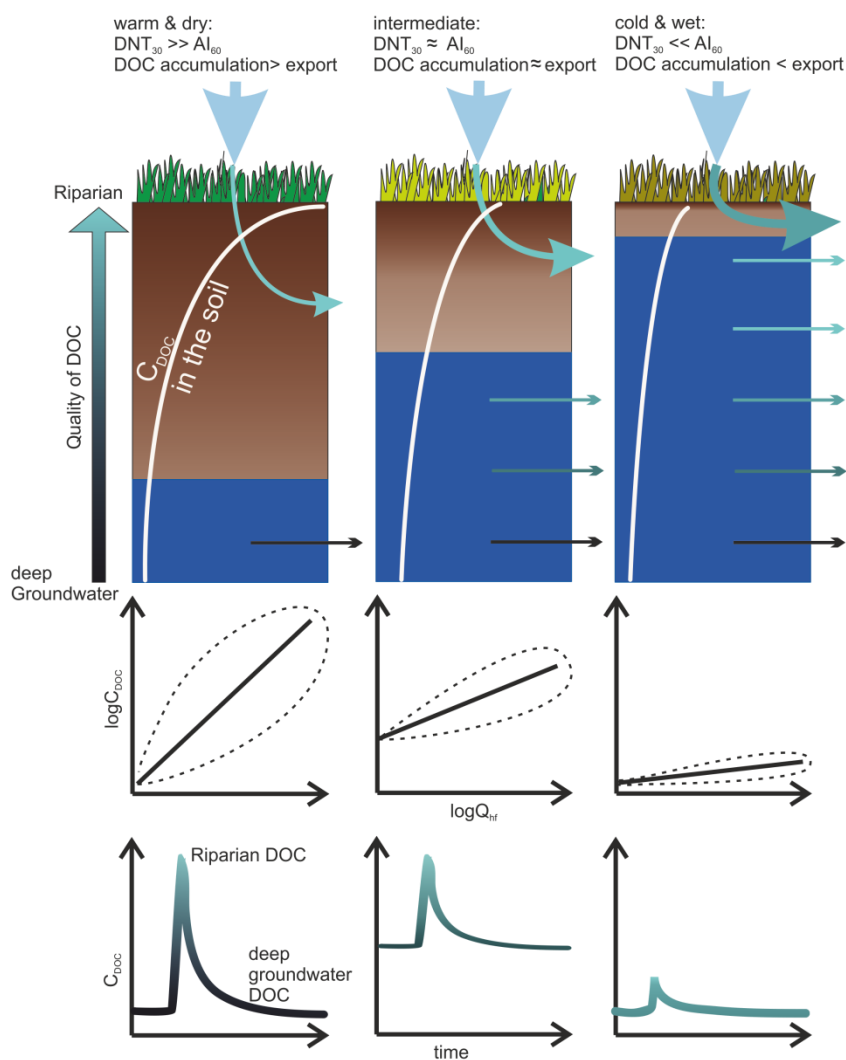
Fig. 6: Conceptual model of riparian DOC export from precipitation during the three hydroclimatic states: warm & dry, intermediate, cold & wet. Depth of the soil column is around 0.5 m. Changing combinations between $SUVA_{254}$ and $S_{275-295}$ values are described as more groundwater influenced (black) and more riparian influenced (green) DOC quality. Arrows indicate the export of DOC, colors of the arrows refer to the respective DOC quality. Panels in the middle row show the relation between C_{DOC} and Q_{hf} during the three situations. Dashed lines indicate the "dispersion" of the point cloud (according R^2) during the events. Panels in the bottom line indicate the change of C_{DOC} during an event. Corresponding changes of colors indicates more groundwater influenced (black) and more riparian influenced (green) DOC quality.

Table 1: Descriptive statistics of DOC and hydroclimatic variables. N refers to number of measurements, St.Dev. – standard deviation, Min – minimum of the measurements, Max – maximum of the measurements and CV – coefficient of variation. Class shows if the variable was utilized as response (r) or predictor (p) in models.

Variable	Description	Class	N	Mean	St. Dev.	Min	Max	Median	CV
C_{DOC} [mg L^{-1}]	DOC concentration	r	42,427	4.60	1.94	1.49	13.05	4.24	0.42
$SUVA_{254}$ [L m^{-1} mg-C^{-1}]	Specific UV absorbance at 254 nm	r	42,427	3.93	0.89	0.68	5.44	4.08	0.23
$S_{275-295}$ [× 10^{-3} nm^{-1}]	Spectral slope between 275 nm and 295 nm	r	42,421	13.59	3.76	2.44	19.98	13.42	0.28
Q_{tot} [m^3 s^{-1}]	Total discharge	-	42,427	0.03	0.07	0.002	1.98	0.01	2.81
Q_{hf} [m^3 s^{-1}]	High-frequency quick flow	p	39,371 [1]	0.02	0.07	0.0001	1.97	0.002	4.51
Q_b [m^3 s^{-1}]	Low-frequency baseflow	p	41,516 [1]	0.01	0.01	0.002	0.06	0.007	0.91
P [mm d^{-1}]	Precipitation	-	42,427	2.21	5.62	0.00	55.50	0.00	2.55
T [°C]	Air temperature	-	42,427	9.20	6.96	-11.75	31.77	9.15	0.76
ET_P [mm d^{-1}]	Potential evapotranspiration	-	20,344	3.01	4.99	0.00	25.98	0.35	1.66
AI_{60}	Aridity Index of the last 60 days	p	17,482	2.73	2.72	0.43	11.33	0.1.43	1.00
DNT_{30} [°C s m^{-3}]	Discharge normalized temperature of the last 30 days	p	42,427	921.37	919.56	-66.20	3,095.86	501.27	1.00
DOC export [g s^{-1}]	DOC export	-	42,427	0.17	0.67	0.005	18.63	0.04	3.88

[1]N of Q_b and Q_{hf} differs from Q_{tot} due to the applied filtering method for baseflow separation.

Table 2: Spearman's rho (r_s) of possible controlling variables over the entire observation period. Only complete cases were used (n = 17,082). All correlations are highly significant (p < 0.001), r_s with absolute values larger 0.6 printed in bold for better readability. Numerical subscripts of T, Q, AI, DNT indicate how many preceding days were aggregated.

	$SUVA_{254}$	S_{275_295}	T	T_{15}	T_{30}	Q_{15}	Q_{30}	AI_6	AI_{14}	AI_{60}	DNT_{30}	Q_{tot}	Q_{hf}	Q_b
C_{DOC}	**0.91**	0.18	0.23	0.30	0.25	0.10	0.03	0.46	0.29	0.11	0.16	0.22	0.49	-0.08
$SUVA_{254}$		0.50	0.13	0.13	0.05	0.22	0.17	0.44	0.26	0.18	-0.05	0.37	0.59	0.08
S_{275_295}			-0.32	-0.53	**-0.63**	0.58	0.56	0.20	0.22	0.47	**-0.66**	**0.67**	0.57	**0.61**
T				**0.70**	0.68	-0.46	-0.51	-0.21	-0.35	-0.56	**0.64**	-0.48	-0.22	**-0.61**
T_{15}					0.96	**-0.60**	**-0.64**	-0.17	-0.39	**-0.71**	**0.85**	**-0.63**	-0.31	**-0.79**
T_{30}						**-0.65**	**-0.68**	-0.15	-0.35	**-0.71**	**0.89**	**-0.66**	-0.34	**-0.81**
Q_{15}							**0.87**	0.33	**0.66**	**0.76**	**-0.80**	**0.80**	0.57	**0.86**
Q_{30}								0.19	0.45	**0.81**	**-0.89**	**0.71**	0.49	**0.79**
AI_6									**0.67**	0.33	-0.18	0.53	**0.60**	0.37
AI_{14}										**0.62**	-0.43	**0.64**	0.56	**0.60**
AI_{60}											**-0.86**	**0.67**	0.47	**0.73**
DNT_{30}												**-0.73**	-0.44	**-0.86**
Q_{tot}													**0.84**	**0.87**
Q_{hf}														0.56

Table 3: Spearman's rho (r_s) of the 38 C_{DOC}, $SUVA_{254}$ and $S_{275-295}$ model coefficients with environmental variables. Asterisks indicate p-values (*** - <0.001, ** - <0.01, * - <0.05), r_s with absolute values larger 0.6 printed in bold.

Model Parameters	T_{15}	T_{30}	Q_{15}	Q_{30}	AI_6	AI_{14}	AI_{60}	DNT_{30}	Q_{hf}	Q_b
z (C_{DOC})	0.07	0.08	-0.08	0.03	0.08	-0.01	-0.09	0.03	0.15	-0.12
a (C_{DOC})	**-0.65** ***	0.44 **	-0.46 *	0.50 **	0.41 *	0.32	**-0.66** ***	**0.63** ***	-0.55 ***	**-0.71** ***
b (C_{DOC})	-0.33 *	0.22	-0.21	0.27	0.22	0.30	-0.15	0.32	-0.38 *	-0.25
z ($SUVA_{254}$)	0.04	0.09	0.09	0.03	0.10	0.01	-0.10	0.04	0.01	-0.09
a ($SUVA_{254}$)	-0.56 ***	0.43 **	-0.50 *	0.50 **	0.40 *	0.34 *	**-0.64** ***	0.58 ***	-0.54 ***	**-0.60** ***
b ($SUVA_{254}$)	-0.34 *	0.13	-0.30	0.21	0.11	0.18	-0.14	0.25	-0.29	-0.23
z ($S_{275-295}$)	0.23	0.02	0.55 *	-0.05	0.00	0.00	0.04	-0.10	-0.02	0.07
a ($S_{275-295}$)	-0.47 **	0.57 ***	-0.54 *	**0.64** ***	0.54 ***	0.47 **	-0.56 ***	**0.62** ***	-0.47 **	**-0.64** ***
b ($S_{275-295}$)	-0.45 **	0.05	-0.56 *	0.13	0.06	0.03	-0.14	0.19	-0.20	-0.24

Table 4: Evaluation of the whole data set model by dropping the least influencing variable according to AIC, starting from the complete models (Eq. (3)).

C_{DOC} model	R^2_{DOC}	$SUVA_{254}$ model	$R^2_{SUVA254}$	$S_{275-295}$ model	$R^2_{S275-295}$
Complete	0.72	Complete	0.64	Complete	0.65
$-\log(Q_{hf}) \times Q_b$	0.71	$-DNT_{30} \times Q_b$	0.60	$-AI_{60} \times DNT_{30}$	0.65
$-DNT_{30} \times Q_b$	0.69	$-\log(Q_{hf}) \times Q_b$	0.56	$-\log(Q_{hf}) \times Q_b$	0.56
$-Q_b$	0.68	$-Q_b$	0.54	$-AI_{60}$	0.54
$-\log(Q_{hf})$	0.42	$-AI_{60} \times DNT_{30}$	0.35	$-DNT_{30} \times Q_b$	0.53
$-AI_{60} \times DNT_{30}$	0.02	$-DNT_{30}$	0.33	$-Q_b$	0.51
$-DNT_{30}$	0.02	$-AI_{60}$	0.31	$-DNT_{30}$	0.23
$-AI_{60}$	0	$-\log(Q_{hf})$	0	$-\log(Q_{hf})$	0